Nucleic Acids Research, 2000, Vol. 28, No. 20 ***4013–4020***

Hammerhead ribozymes selectively suppress mutant type I collagen mRNA in osteogenesis imperfecta fibroblasts

Paul A. Dawson and Joan C. Marini*

Section on Connective Tissue Disorders, Heritable Disorders Branch, NICHD, National Institutes of Health, Bethesda, MD 20892, USA

Received May 17, 2000; Revised August 9, 2000; Accepted August 20, 2000

ABSTRACT

Ribozymes are a promising agent for the gene therapy of dominant negative genetic disorders by allele-specific mRNA suppression. To test allele-specific mRNA suppression in cells, we used fibroblasts from a patient with osteogenesis imperfecta (OI). These cells contain a mutation in one α1(I) collagen allele which both causes the skeletal disorder and generates a novel ribozyme cleavage site. In a preliminary *in vitro* assay, ribozymes cleaved mutant RNA substrate whereas normal substrate was left intact. For the studies in cell culture we generated cell lines stably expressing active (AR) and inactive (IR) ribozymes targeted to mutant α1(I) collagen mRNA. Quantitative competitive RT–PCR analyses of type I collagen mRNA, normalized to β-actin expression levels, revealed that the level of mutant α1(I) collagen mRNA was significantly decreased by ~50% in cells expressing AR. Normal α1(I) collagen mRNA showed no significant reduction when AR or IR was expressed from the pHβAPr-1-neo vector and a small (10–20%) but significant reduction when either ribozyme was expressed from the pCI.neo vector. In clonal lines derived from cells expressing AR the level of ribozyme expression correlated with the extent of reduction in the mutant:normal α1(I) mRNA ratio, ranging from 0.33 to 0.96. Stable expression of active ribozyme did not affect cell viability, as assessed by growth rates. Ribozyme cleavage of mutant mRNA results in a reduction in mutant type I collagen protein, as demonstrated by SDS–urea–PAGE. This is the first report of ribozymes causing specific suppression of an endogenous mutant mRNA in cells derived from a patient with a dominant negative genetic disorder.

INTRODUCTION

Osteogenesis imperfecta (OI) is a dominantly inherited disorder of connective tissue, with phenotypes ranging from perinatal lethal to clinically mild (1,2) and an incidence of 1/10 000–20 000 live births. OI has frequently served as a model disorder for dominant negative conditions of structural proteins. All types of OI are caused by mutations in type I collagen, the major structural component of bone and skin extracellular matrix, and all types have osteopenia and susceptibility to fracture. Because OI is a generalized disorder of connective tissue, affected individuals may die in the perinatal period from respiratory causes (type II OI) or may endure varying degrees of significant physical handicap, extreme growth deficiency, scoliosis, cor pulmonale, basilar invagination and an ultimately reduced lifespan (types III and IV OI). Individuals with the clinically significant types II–IV OI have structural defects in either the α1 or α2 chains that comprise the type I collagen helix. The majority of these structural defects are caused by point mutations that result in the substitution of a glycine residue by an amino acid with a bulkier side chain (3). Individuals with the clinically very mild type I OI almost invariably have a null allele for the α1(I) chain, producing normal collagen in reduced amounts (4).

Conventional therapies can result in a more functional life for severely affected individuals but have a limited impact on long-term complications (2). The gene therapy approach for this disorder, and other dominant negative disorders, poses special challenges. Gene therapy for recessive disorders involves the replacement of a missing or defective gene. Even partial enzyme replacement would be anticipated to reverse symptoms. For dominant negative disorders, the mutant protein is synthesized and actively exerts a detrimental effect in spite of the presence of the normal product made by the normal allele. For these disorders a suppression approach to therapy is logical, in which an agent would selectively inactivate expression of the mutant type I collagen allele without affecting expression from the normal allele. If the process were fully efficient it would convert a mutant allele into a null allele. Based on the genotype/phenotype correlation of type I OI, suppression of mutant RNA should modulate the severity of OI without causing adverse consequences.

*To whom correspondence should be addressed at: Building 10, Room 9S241, 10 Center Drive, MSC 1830, Bethesda, MD 20892-1830, USA.
Tel: +1 301 496 6683; Fax: +1 301 402 0234; Email: oidoc@helix.nih.gov
Present address:
Paul A. Dawson, Department of Physiology and Pharmacology, University of Queensland, Brisbane, Australia

One approach to mutation suppression involves the use of antisense technologies to inactivate the mutant mRNA. Antisense oligonucleotides have been used to inhibit the expression of a mutant α2(I) allele in cultured fibroblasts derived from a patient with type IV OI (5). That investigation demonstrated the suppression of mutant protein to ~50% and mutant α2(I) mRNA to ~40% of their levels in control cells. However, the antisense oligonucleotides also suppressed the normal allele mRNA to 80% of its level in untreated cells. Unfortunately, the specificity of mutant allele suppression observed in the antisense oligonucleotide experiments appears to be insufficient for therapeutic trials.

Ribozymes represent an alternative agent for allele-specific inactivation of mutant mRNAs. Hammerhead ribozymes are the smallest form of catalytic RNA which can be designed to cleave almost any RNA (6). The combination of requirements for both a cleavage site and a binding site provide ribozymes with specificity capabilities for point mutations that cannot be achieved with linear antisense oligonucleotides. In addition, the catalytic capacity of the ribozyme provides the potential for increased efficiency and stability. Ribozymes have been used to cleave viral (HIV and influenza) and cellular RNAs *in vitro* and *in vivo* (7–10). Studies on Marfan syndrome, another dominant negative genetic disorder, demonstrated that ribozymes efficiently cleaved fibrillin RNA in cultured fibroblasts (11) and osteosarcoma cells (12). However, cleavage in these situations was not designed to be allele specific. Mutation-specific cleavage of transgene opsin mRNA in rat (13) and of N-ras mRNA *ex vivo* (14) suggests that ribozymes can be used to selectively suppress the expression of one allele *in vivo*. For OI ~25% of the causative type I collagen point mutations also generate a novel ribozyme cleavage site (6). Thus, the mutation itself provides the target for mutant RNA suppression.

Previously we reported the selective cleavage of mutant type I collagen RNAs in cell-free assays using hammerhead ribozymes (15). In the present study we report the efficiency and specificity of hammerhead ribozymes in cultured OI fibroblasts. We targeted mutant α1(I) collagen mRNA, containing a single base mutation that generates a ribozyme cleavage site. This is the first report of ribozymes effecting allele- and mutation-specific mRNA suppression in cultured cells. These findings are promising for future development of ribozymes as agents for the gene therapy of dominant negative genetic disorders, such as OI.

MATERIALS AND METHODS

Cell culture and transfection

Dermal fibroblasts from an OI patient, G85V (16), were cultured in Dulbecco's modified Eagle's medium (DMEM) (Gibco BRL, Grand Island, NY) supplemented with 10% fetal calf serum. Cells were plated in 6-well plates and transfected at ~70% confluency. Cells were transfected for 3.5 h at 37°C with fresh serum-free medium containing 0.14 nM premixed plasmid DNA and 2 μg/ml cationic lipid (LipofectAMINE; Gibco BRL). Post-transfection the medium was replaced with 2 ml of DMEM supplemented with 10% fetal calf serum. Transfected cells were selected by addition of 0.4 mg/ml G418 (Gibco BRL) for 3 weeks. Stable cell lines were maintained in medium containing 0.2 mg/ml G418. Clonal cell lines were generated by plating stably transfected cells in 96-well plates and culturing in F10 medium (Zazo Diagnostic Laboratories, Lexington, KY) supplemented with 10% fetal calf serum and 0.4 mg/ml G418.

To determine cell growth rates, untransfected and stably transfected (pCI.neo vectors) cells were plated in triplicate at a density of 5×10^3 cells/well of a 24-well plate in DMEM supplemented with 10% fetal calf serum. Cells were trypsinized and counted at various times over a period of 11 days. Linear analyses of growth rates were performed using a normal *Z*-test.

Construction of plasmids

For *in vitro* experiments we prepared plasmids encoding substrate RNA. Inserts of 226 bp containing 117 bp of α1(I) collagen cDNA derived from the G85V cell line and 109 bp of flanking vector sequence were amplified by PCR using the primer pair 85S1 and 85AS1 (Table 1). The PCR products were ligated into vector pCR2.1 (Invitrogen, Carlsbad, CA). Inserts were sequenced and the orientation verified. For plasmids encoding ribozymes, two complementary oligodeoxynucleotides were synthesized for each ribozyme construct. The sequences of the oligodeoxynucleotides, containing *Sal*I sites on both the 5′- and 3′-termini (lower case), the catalytic core (bold sequence) and 13 nt binding arms, are shown in Table 1. Two base changes in the highly conserved catalytic core sequence (underlined bases) were introduced to generate inactive ribozymes (IR). Aliquots (4 μg) of each primer pair (sense and antisense) were mixed in 1× PCR Buffer II (Perkin Elmer-Cetus, Norwalk, CT) to a final volume of 50 μl. The primers were denatured by heating to 95°C for 4 min and annealed by slow cooling to 20°C over 1 h. The fragments were digested with *Sal*I (Gibco BRL) and ligated into the *Sal*I site of the mammalian expression vectors pCI.neo (Promega, Madison, WI) and pHβAPr-1-neo (a gift from Dr L. H. Kedes, Department of Biochemistry, University of Southern California) to produce plasmids pCI.neo/AR, pCI.neo/IR, pHβAPr-1-neo/AR and pHβAPr-1-neo/IR. In the pCI.neo vector, ribozyme sequences were placed downstream of the human CMV immediate early enhancer/promoter region and an intron element (comprising the 5′-donor site from the first intron of the human β-globin gene and the branch and 3′-acceptor site from the intron of an immunogloubulin gene heavy chain variable region) and upstream of the SV40 late polyadenylation site. The pCI.neo vector also contains T7 and T3 RNA polymerase promoters that flank the ribozyme sequences. In the pHβAPr-1-neo vector, ribozyme sequences were cloned downstream of the human β-actin promoter plus 5′-UTR and intervening sequence 1 (IVS1) and upstream of the SV40 late polyadenylation signal. The pCI.neo and pHβAPr-1-neo vectors are predicted to generate ribozyme-containing transcripts of 552 and 1123 nt, respectively, plus an additional poly(A) tail. Plasmid DNA was prepared using an EndoFree Plasmid Maxi Kit (Qiagen, Santa Clarita, CA). Sequence and orientation of the ribozyme templates was verified.

For plasmids containing competitor sequences for quantitative PCR, oligonucleotides were synthesized (Table 1) to generate competitor templates of β-actin, ribozyme and α1(I) collagen cDNA using PCR. Each competitor template contains an additional 20 nt artificial sequence (lower case italic in Table 1)

Table 1. Primers used in construction of templates and competitors

Oligos for constructing β-actin competitor	
BA1.S	5′-CATGTGCAAGGCCGGCTTCG-3′
BA2.AS	5′-*ctcgacggatccctgcaggt*CCTGGTGCCTGGGGCGCCCCA-3′
BA3.S	5′-*acctgcagggatccgtcgag*GGCGTGATGGTGGGCATGGG-3′
BA4.AS	5′-GAAGGTGTGGTGCCAGATTT-3′
Oligos for constructing α1(I) substrate and α1(I) collagen competitor	
85S1	5′-TCAGGGTGCTCGAGGATTGCCCGGAACAG-3′
85AS2	5′-*ctcgacggatccctgcaggt*GGGAGGCCAGCTGTTCCG-3′
85S2	5′-*acctgcagggatccgtcgag*TGGAATGAAGGGACACAG-3′
85AS1	5′-TCACCCTTAGGACCAGCAGGACCAGCATCTC-3′
Oligos for constructing pCI.neo ribozyme competitor and detecting ribozyme	
RZ1.1S	5′-ACGACTCACTATAGGCTAGC-3′
RZ1.S	5′-ACGACTCACTATAGGCTAG-3′
RZ2.AS	5′-*ctcgacggatccctgcaggt*AACCCTCACTAAAGGGAAG-3′
RZ3.S	5′-*acctgcagggatccgtcgag*AATGCTTCGAGCAGACATGA-3′
RZ4.AS	5′-TTTGTCCAAACTCATCAATG-3′
Oligos for constructing pHβAPr-1-neo ribozyme competitor and detecting ribozyme	
RZ5.S	5′-AGGACTCGGCGCGCCGGAAG-3′
RZ6.AS	5′-*ctcgacggatccctgcaggt*GGGCGCGCTGTGAGCCGAAG-3′
RZ7.S	5′-*acctgcagggatccgtcgag*GGCTATTCTCGCAGGATC-3′
RZ8.AS	5′-GTCTGGATCCCTCGAAGCTTG-3′
Oligos for constructing ribozyme templates	
AR85S	5′-caacgcgtcgacTGTGTCCCTTCAT**CTGATGAGTCCGTGAGGACGAA**ACAGGGAGGCCAGgtcgacaagcac-3′
AR85AS	5′-gtgcttgtcgacCTGGCCTCCCTGT**TTCGTCCTCACGGACTCATCAG**ATGAAGGGACACAgtcgacgcgttg-3′
IR85S	5′-caacgcgtcgacTGTGTCCCTTCAT**CTAATGAGTCCGTGAGGACGAGA**CAGGGAGGCCAGgtcgacaagcac-3′
IR85AS	5′-gtgcttgtcgacCTGGCCTCCCTGT**CTCGTCCTCACGGACTCATTAGA**TGAAGGGACACAgtcgacgcgttg-3′

Lower case italic sequences are artificial 20 nt sequence in competitor oligos, lower case non-italic sequences contain *Sal*I restriction sites. Bold sequences represent the ribozyme catalytic core. S, sense oligo; AS, antisense oligo; AR, active ribozyme; IR, inactive ribozyme.

which allows the electrophoretic separation of amplified endogenous cDNA from competitor cDNA. All competitor templates were cloned into vector pCR2.1 (Invitrogen) and sequences and orientation were verified. For construction of the β-actin competitor template, primer pairs BA1.S + BA2.AS and BA3.S + BA4.AS were used to amplify 100 and 166 bp segments, respectively, of β-actin cDNA. Aliquots (1 µl) of each PCR product were added to a second round PCR to amplify a 246 bp competitor template using primers BA1.S and BA4.AS under the same conditions. For construction of the pCI.neo and pHβAPr-1-neo ribozyme competitor templates, primer pairs RZ1.S + RZ2.AS and RZ3.S + RZ4.AS were used to amplify 105 and 66 bp segments, respectively, of pCI.neo vector sequence using the conditions described for the β-actin competitor. Aliquots (1 µl) of the PCR products were combined and a 151 bp fragment was amplified using primers RZ1.S and RZ4.AS. The same procedure was used to generate a 132 bp competitor template of pHβAPr-1-neo/ribozyme using the pHβAPr-1-neo vector as template and primers RZ5.S, RZ6.AS, RZ7.S and RZ8.AS. For construction of the α1(I) collagen competitor template, primers 85S1, 85AS2, 85S2 and 85AS1 were used to PCR amplify a 138 bp α1(I) cDNA fragment derived from OI G85V cells. The α1(I) collagen competitor template includes the G907→T mutation. The competitor constructs are designated BAC (β-actin competitor), pCRZC (pCI.neo/ribozyme competitor), pβRZC (pHβAPr-1-neo/ribozyme competitor) and α1C [α1(I) collagen competitor for OI G85V cells].

In vitro transcription and ribozyme cleavage

Vectors containing substrate or ribozyme templates were linearized with *Bam*HI or *Not*I, respectively. All transcripts were generated with T7 RNA polymerase (Promega). Substrate transcripts were labeled by incorporation of [α-^{32}P]UTP (800 Ci/mmol; Amersham Pharmacia Biotech, Cleveland, OH). Specific activity of the [α-^{32}P]UTP and the base composition of each substrate molecule were used to calculate the substrate concentration. Ribozyme transcripts were quantified spectrophotometrically.

Cleavage reactions contained 1 nM substrate RNA, increasing amounts (1–50 nM) of ribozyme, 20 mM $MgCl_2$ and 50 mM Tris–HCl, pH 8.0, in a final volume of 10 µl.

Substrates and ribozymes were denatured at 95°C for 30 s, then chilled on ice. Cleavage reactions were initiated by the addition of $MgCl_2$ and were incubated for 2 h at 50°C. Reactions were stopped by addition of loading buffer (80% formamide, 10 mM Na_2EDTA, pH 8.0, and 1 mg/ml each bromophenol blue and xylene cyanol). Cleavage products were analyzed on 10% polyacrylamide–7 M urea gels. Product and substrate fragments were quantitated by densitometry analysis using a Fuji phosphorimager.

RNA extraction and amplification

Prior to RNA extraction cells were incubated in G418-free medium for 48 h. RNA was isolated using TriReagent (Molecular Research Center, Cincinnati, OH) according to the manufacturer's protocol, then treated with 1 U RQ1 RNase-free DNase (Promega) for 15 min at 37°C and purified using an RNeasy Total RNA kit (Qiagen).

To detect ribozyme expression in cells, 100 ng of total RNA was RT–PCR amplified using 0.25 µM each primer: RZ1.1S + RZ4.AS for pCI.neo/ribozyme; RZ5.S + RZ8.AS for pHβAPr-1-neo/ribozyme. Amplified pCI.neo/ribozyme and pCI.neo vector alone yield fragments of 341 and 287 bp, respectively. Amplified pHβAPr-1-neo/ribozyme and pHβAPr-1-neo vector alone yield fragments of 168 and 114 bp, respectively. PCR products were resolved on a 1.5% agarose gel in 1× TBE, stained with ethidium bromide and visualized under UV light.

A quantitative competitive RT–PCR protocol was designed for quantitation of ribozyme, β-actin and normal and mutant type I collagen expression. Competitor RNAs were co-amplified with each of the endogenous transcripts. They were transcribed using *Hin*dIII-linearized plasmid constructs and T7 RNA polymerase in the presence of [α-^{32}P]UTP. Their concentration was calculated from the specific activity and the number of UTPs per molecule.

Reverse transcriptase reactions were performed in a total volume of 10 µl using 10 ng total RNA, serially diluted competitor RNA (β-actin, 5×10^5–10^4 molecules; RZ, 5×10^6–10^5 molecules; α1(I) collagen, 10^6–5×10^4 molecules), 1× PCR Buffer II (Perkin Elmer-Cetus), 2.5 mM $MgCl_2$, 12.5 U MuLV reverse transcriptase, 0.25 mM each dNTP, 5 U RNase inhibitor and 0.625 µM antisense primer BA4.AS, RZ4.AS, RZ8.AS or 85AS1. PCRs were performed in a total volume of 25 µl using 10 µl cDNA, 2 mM $MgCl_2$, 1 µCi [α-^{32}P]dCTP (3000 Ci/mmol; Amersham Pharmacia Biotech), 1× PCR Buffer II and 0.5 U AmpliTaq Gold (Perkin Elmer-Cetus) and 0.5 µM each primer pair BA1.S + BA4.AS (β-actin), RZ1.S + RZ4.AS (pCI.neo ribozyme), RZ5.S + RZ8.AS (pHβAPr-1-neo ribozyme) and 85S1 + 85AS1 [α1(I) collagen]. Co-amplified β-actin and competitor cDNA yield fragments of 226 and 246 bp, respectively. Co-amplified pCI.neo/ribozyme and competitor yield fragments of 187 and 151 bp, respectively. Co-amplified pHβAPr-1-neo/ribozyme and competitor yield fragments of 168 and 132 bp, respectively. Restriction endonuclease digestions were performed to separate amplified normal and mutant type I collagen cDNAs. The amplified α1(I) product was digested for 16 h with *Bst*NI. The digested samples were desalted, concentrated using a microcon-10 spin column (Amicon, Beverly, MA) and electrophoresed on 10% polyacrylamide gels. The normal α1(I) collagen cDNA was cleaved, yielding 78 and 39 bp fragments, whereas the competitor and mutant α1(I) collagen cDNA were not cleaved, yielding 137 and 117 bp fragments, respectively. The radioactivity of the bands was quantified by densitometry analysis using a Fuji phosphorimager. The amount of mRNA in each sample was calculated by plotting the logarithm of the ratio of the target band to the competitor band against the logarithm of the corresponding number of molecules of the competitor. When the ratio is equal to 1, the initial amount of unknown RNA is equivalent to the amount of competitor. Each quantitative-competitive (QC) RT–PCR assay was performed in triplicate and the *P* values were calculated using an unpaired *t*-test in the MS Excel program.

Collagen protein studies

Dermal fibroblasts were incubated with 3.75 µCi [^{14}C]proline (250 mCi/mmol; Amersham Pharmacia Biotech) at 37°C for 3 h. Type I procollagen was precipitated from the cell layer (17). Collagens were prepared by digestion with pepsin (100 µg/ml) for 3 h at 15°C and analyzed by SDS–urea–PAGE (15). To quantitate the radioactivity of individual collagen chains, bands were excised from the gel, digested in 1 ml of tissue solubilizer (TS-2; Research Products Information Corp., Mount Prospect, IL) and the radioactivity measured by scintillation counting. This analysis was performed in triplicate on independent collagen preparations from OI cells.

RESULTS

Ribozyme cleavage *in vitro*

In order to develop a gene therapy approach for OI, we selected a type I collagen mutation which not only causes an OI phenotype, but also generates a novel ribozyme cleavage site. The mutation selected is a 907G→T change at codon 85 (Gly85→Val) in α1(I) collagen mRNA which creates a novel GUA ribozyme cleavage site. Thus, the mutation itself provides the target for allele-specific cleavage of mutant collagen mRNA. We designed hammerhead ribozymes with 13 nt binding arms to target this site, containing an active or inactive catalytic core (Fig. 1). To confirm the activity of the ribozyme and the accessibility of the target site, preliminary *in vitro* experiments were performed (data not shown). Synthetic ^{32}P-labeled RNA transcripts, containing 117 nt segments of either normal or mutant α1(I) mRNA and 109 nt of flanking vector sequence, were incubated with active or inactive ribozyme as described in Materials and Methods. Only the active ribozyme cleaved mutant substrates into the expected 111 and 115 nt fragments. In this assay 17% of mutant substrate was cleaved at an active ribozyme:substrate ratio of 1:1 and >75% of target was cleaved at a 50:1 ratio.

Ribozyme cleavage in OI cells

For the studies in cultured cells we cloned inactive and active ribozyme templates into the mammalian expression vectors pCI.neo and pHβAPr-1-neo. Using selection with G418, we were able to generate cells stably expressing active ribozymes, inactive ribozymes or vector sequences alone for both vectors. Expression of ribozymes and vector sequence alone was detected by RT–PCR analysis (Fig. 2, lanes 5–7). Primer pairs used in this PCR were located within the vector outside the cloned ribozyme sequence and are designed to amplify both vector alone and vector containing ribozyme. Products of 341

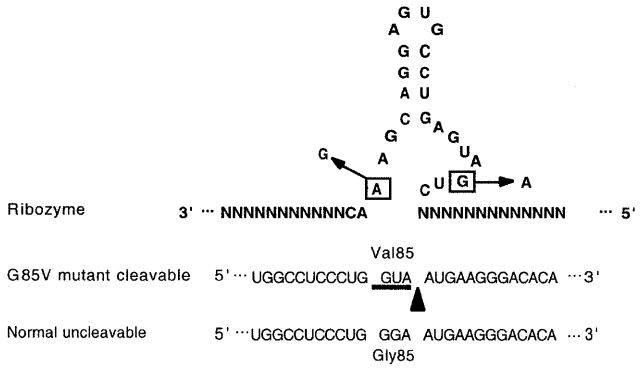

Figure 1. Hammerhead ribozyme structure and partial sequence of the α1(I) collagen RNA substrate. The targeted GUA cleavage site is underlined in the mutant sequence and the cleavage site is indicated by an arrowhead. The base changes in the inactive ribozyme are boxed.

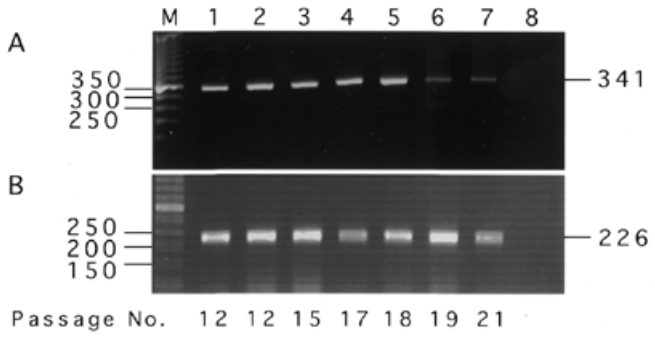

Figure 3. Detection of ribozyme expression with increasing cell passages. Ethidium bromide stained gels showing RT–PCR amplified (**A**) pCI.neo/active ribozyme and (**B**) β-actin cDNA using G85V total RNA from passages 12–21. Lane M contains a 50 bp molecular weight ladder DNA. Lane 8 is a negative control. The sizes of the fragments are indicated on the right.

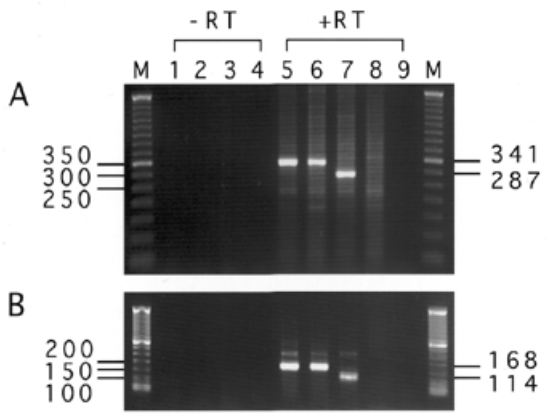

Figure 2. RT–PCR detection of ribozyme expression in G85V cells stably transfected with (**A**) pCI.neo and (**B**) pHβAPr-1-neo expression vectors. Ethidium bromide stained agarose gels contain amplified active ribozyme (341 and 168 nt), inactive ribozyme (341 and 168 nt) and vector cDNA (287 and 114 nt) (lanes 5–7, respectively). Lanes 1–4 contain samples without reverse transcriptase (RT) and correspond to lanes 5–8. Lanes 8 and 9 represent untransfected and negative control samples, respectively. Lane M contains a 50 bp molecular weight ladder DNA. The sizes of the fragments are indicated on the right.

and 168 bp were detected in samples expressing ribozyme from pCI.neo and pHβAPr-1-neo, respectively. Amplification of these empty vectors yielded 287 and 114 bp products, respectively. The absence of PCR products in the samples not containing reverse transcriptase (Fig. 2, lanes 1–4) confirmed that the amplified products were derived from an RNA template and not DNA contamination. The expression of active ribozymes from the pCI.neo vector was detected in G85V cells for multiple passages following transfection. There was a decrease in the level of amplified ribozyme cDNA in cell passages higher than P18 (Fig. 3), presumably due to either loss of expression cassette or CMV promoter attenuation.

Our next goal was to demonstrate the efficiency and specificity of the ribozymes expressed in stably transfected cells. The ability of ribozymes to specifically cleave mutant α1(I) collagen mRNA in cells was evaluated using a QC RT–PCR assay (Fig. 4). The α21(I) collagen mutation selected for this study not only generates a GUA ribozyme cleavage site, but also deletes a *Bst*NI site. Thus, *Bst*NI digestion of PCR-amplified α1(I) cDNAs allows the electrophoretic separation of normal and mutant products. Levels of normal and mutant type I collagen mRNA and ribozyme were normalized to β-actin mRNA levels. The G85V cells stably expressing active ribozyme from either the pCI.neo or pHβAPr-1-neo vector had substantially decreased levels of mutant α1(I) mRNA levels relative to untransfected cells or cells transfected with vector alone (Table 2). The G85V cells expressing pCI.neo/active ribozyme had a 53 ± 5% decrease in mutant α1(I) level and those expressing pHβAPr-1-neo/active ribozyme had a 57 ± 8% decrease relative to untransfected cells. These levels of mutant α1(I) mRNA suppression were achieved with ribozyme:total α1(I) mRNA ratios of 3–5:1 and 12–14:1, respectively.

The level of normal α1(I) mRNA was unchanged when active or inactive ribozyme was expressed from the pHβAPr-1-neo vector. The same ribozymes expressed from the pCI.neo vector did cause a small (10–20%) but significant reduction in normal mRNA levels. These data suggest that the expressed sequences surrounding the ribozyme may play a role. For the pCI.neo transcript this includes 184 nt of pGEM-3Zf sequence, the T7 promoter and vector cloning site at the 5′-end of the transcript and the T3 promoter and SV40 polyadenylation signal. These sequences contain no significant homology to the region of α1(I) cDNA flanking the cleavage site. The transcript from pHβAPr-1-neo is twice as long as that from pCI.neo and the presence of longer tails on both sides of the ribozyme might result in faster cycling of ribozyme off target, minimizing an antisense effect.

Ribozyme cleavage in clonal cell lines

Since the experiments described above used a mixed population of stably transfected cells, the calculated values are averages of the cell pool. To test for potential variations in the level of pCI.neo/active ribozyme expression and to determine if such variation would correlate to the degree of mutant α1(I) mRNA cleavage, G85V clonal lines were generated. RNA was collected from single wells of a 96-well plate and used for RT–PCR analyses (Fig. 5). Three of the clonal lines expressed higher

Table 2. Levels of mutant and normal α1(I) collagen mRNA in G85V cells, normalized to β-actin mRNA

Cell line	Normal α1(I)/β-actin				Mutant α1(I)/β-actin			
	%UT	*P* values			%UT	*P* values		
		UT	V	IR		UT	V	IR
Untransfected	100				100			
pCI.neo	89 ± 10				91 ± 8			
pCI.neo/IR	89 ± 5	0.03			89 ± 3	0.01		
pCI.neo/AR	78 ± 10	0.03	0.004	0.05	47 ± 5	0.001	0.001	0.002
Untransfected	100				100			
pHβAPr-1-neo	104 ± 11				98 ± 13			
pHβAPr-1-neo/IR	90 ± 10				97 ± 14			
pHβAPr-1-neo/AR	89 ± 12				43 ± 8	0.003	0.02	0.005

Values are averages of experiments performed in triplicate. For each set of cells *P* values were calculated relative to each other set. Only significant *P* values are shown. UT, untransfected cells; V, vector; IR, inactive ribozyme; AR, active ribozyme.

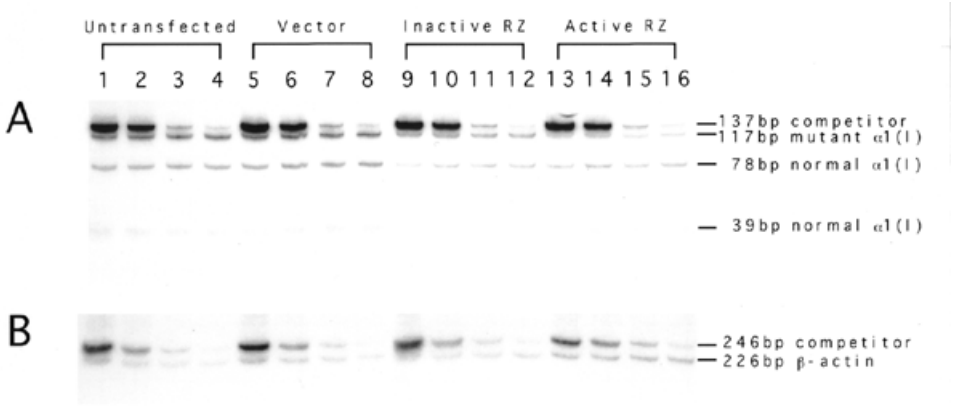

Figure 4. QC RT–PCR assay of α1(I) collagen mRNA derived from G85V stably transfected (pCI.neo vectors) cells. Separation of (**A**) competitor from normal and mutant α1(I) collagen products following digestion with *Bst*N1 and (**B**) competitor from β-actin products on 10 and 6% polyacrylamide gels, respectively. The sizes of the fragments are indicated on the right. Each set of four lanes, containing serially diluted competitor sample, was used to calculate a single value of target molecule number.

levels of ribozyme (Fig. 5, lanes 5–7). These lines also showed marked reduction in the ratio of mutant to normal α1(I) mRNA (0.33–0.41). Two clonal lines (Fig. 5, lanes 3 and 4) had both undetectable ribozyme expression and unreduced levels of mutant collagen mRNA [ratio mutant:normal α1(I), 0.95–0.96]. We noted that all transfected cells have a reduced amount of collagen RT–PCR products as compared to untransfected cells. Since the clonal lines were derived with vector pCI.neo, there may also be some reduction in the relative amount of normal collagen transcript. Clonal lines were not derived from transfected normal cells and the potential antisense effect in this experiment was not quantitated.

Effect of ribozyme expression on type I collagen protein

Finally, the capacity of the pCI.neo/active ribozyme to reduce the level of mutant α1(I) collagen protein was investigated. The G85V substitution generates a pepsin-sensitive site in the type I procollagen helix. Following digestion with pepsin, truncated α1 chains are generated and detected by SDS–urea–PAGE (Fig. 6). In triplicate samples of untransfected OI cells and OI cells transfected with active ribozyme, we examined the effect of ribozyme on the level of truncated α1 chain. Only cells expressing active ribozyme were tested, because cells with inactive ribozyme had unreduced levels of α1(I) transcripts. Since the pepsin-sensitive site is not quantitatively cleaved, the overexposed gels required to detect the mutant chains radiographically were unsuitable for densitometry (Fig. 6B). Chains were instead quantitated using direct counts of solubilized bands. Cells expressing active ribozyme had a ratio truncated α1:normal α1 that was reduced to 70 ± 12% of the ratio in untransfected cells. The lack of significant homology of the ribozyme to α2 mRNA sequences makes a decrease in α2 mRNA unlikely. Furthermore, because of the fixed $\alpha1(I)_2\alpha2(I)$ composition of type I collagen, this assay is only sensitive to the relative amounts of the normal and mutant forms of α1. As expected, the α1:α2 ratio was 1.97 in untransfected OI cells and 2.07 in transfected cells.

Effect of ribozyme on cell growth

To examine whether stably expressed active ribozyme affects cell viability, we investigated the effect of the pCI.neo/active ribozyme on the growth rate of G85V cells. Under subconfluent

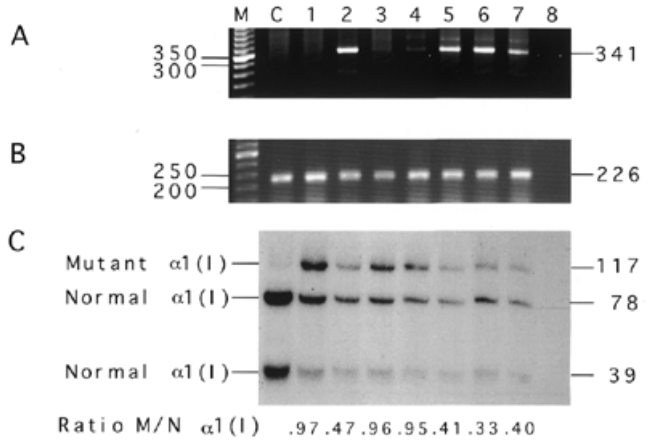

Figure 5. Analysis of ribozyme and α1(I) collagen mRNA levels in clonal G85V stable cell lines. Ethidium bromide stained gels showing amplified (**A**) pCI.neo/active ribozyme and (**B**) β-actin cDNA. (**C**) Radiograph showing *Bst*NI-digested, PCR-amplified α1(I) collagen products; the ratios mutant:normal α1(I) collagen products are indicated at the bottom. Lane C is a normal control cell line; lanes 1–7 represent untransfected, pooled transfected and clones 1–5 of G85V stable cells, respectively. Lane 8 is a negative control. Lane M contains a 50 bp molecular weight ladder DNA. The sizes of the fragments are indicated on the right. The lanes in (A) correspond to the same samples used for RT–PCR in (B) and (C).

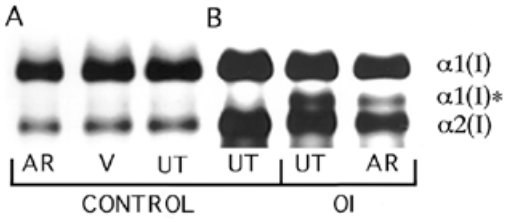

Figure 6. SDS–urea–PAGE of pepsin-treated collagens from stably transfected fibroblasts. (**A**) Collagens from normal control cells; (**B**) collagens from control and G85V cells. The gel in (B) is overexposed to show the truncated chain. Cells were untransfected (UT), transfected with pCI.neo vector alone (V) or transfected with pCI.neo-active ribozyme construct (AR). Truncated α1(I) collagen chains are generated by cleavage at a pepsin-sensitive site and are denoted by an asterisk.

conditions the transfected cells displayed an initial delay in growth (days 2–5). However, after this lag time there was no significant difference in cell growth rate between untransfected cells (cell doubling 3.5 ± 0.3 days) and cells stably transfected with pCI.neo vector (cell doubling 4.4 ± 0.7 days,), pCI.neo/IR (cell doubling 3.2 ± 0.3 days) or pCI.neo/AR (cell doubling 4.4 ± 0.7 days), indicating that expression of the G85V-specific active ribozyme is not detrimental to cell viability.

DISCUSSION

For dominant negative genetic disorders, such as OI, the goal of gene therapy is to selectively inactivate the mutant allele without affecting normal allele expression. OI is well suited to selective suppression of mutant allele expression since a null α1(I) collagen allele is associated with a mild clinical phenotype. Furthermore, a significant proportion (>25%) of all type I collagen point mutations generate a ribozyme cleavage site. In addition, a polymorphic site in COL1A1 with a heterozygosity frequency of 0.4 has recently been demonstrated to undergo efficient allele-specific ribozyme cleavage *in vitro* (18). This provides an alternative suppression target to the mutation itself for OI patients whose collagen mutation occurs in COL1A1, who are heterozygous for the polymorphism and whose mutation occurs on the allele with the cleavable form of the polymorphism. Combining direct mutation suppression and polymorphism-linked suppression, ~35–40% of OI cases could be targeted by ribozymes.

In the present study we report the use of hammerhead ribozymes targeted to a GUA cleavage site on mutant α1(I) collagen RNA. This cleavage site is generated by a disease-causing point mutation (G907→T), previously detected in a patient with OI (15). Thus, the mutation itself provides the target for mutant RNA suppression. We first analyzed the ribozymes in cell-free assays using short, uniformly labeled α1(I) substrate RNA and transcripts of active and inactive ribozyme. The active ribozymes were able to effectively cleave the mutant substrate RNA molecules into products of the expected size. Normal transcripts were uncleaved, although they contain an intact binding site, demonstrating the absolute requirement for a cleavage site. Ribozymes which were stably transfected in cultured OI fibroblasts also had the ability to selectively reduce the level of mutant α1(I) collagen mRNA. Our QC RT–PCR assays revealed a substantial reduction (~50%) in the level of mutant α1(I) mRNA in pooled cells expressing active ribozyme at a 3–14:1 ratio of ribozyme to target RNA molecule. Analysis of individual clonal lines, derived from cells expressing active ribozyme, showed a range of ribozyme expression levels, presumably due to the copy number and/or the chromosomal location of the ribozyme construct. This range in ribozyme expression level corresponded to the level of mutant α1(I) mRNA. Thus, high level ribozyme expression appears to be necessary to attain >50% levels of mutant α1(I) collagen mRNA suppression.

We also demonstrated the capacity of the active ribozyme to reduce the level of mutant α1(I) protein. In OI cells expressing active ribozyme we observed a 30 ± 12% reduction in the ratio pepsin-truncated:normal α1 chains. Unfortunately, cleavage at a pepsin-sensitive site in the collagen helix provides an estimate of the amount of mutant chain present, rather than a quantitative assay. In fact, the calculated ratio probably underestimates the true ratio mutant:normal α1 chains. Since the pepsin-sensitive site generated by the mutation fails to be cleaved in all helices containing mutant chain, it is reasonable to postulate a difference in the pepsin cleavage efficiency of collagen helices with either one or two mutant (G85V) α1 chains. By random distribution of α1 chains into helices, a 50% decrease in mutant α1(I) mRNA would lead to a disproportional decrease in helices containing two mutant chains, from 1/3 to approximately 1/5 of mutation-containing helices. This change in distribution of helix composition would compromise our ability to detect the total decrease in pepsin-cut mutant α1 chain. Finally, stable expression of the active ribozyme had no detrimental effect on cell growth rate. Taken together, these data demonstrate the potential of ribozymes as therapeutic agents for allele-specific suppression in the cellular environment.

In a clinical setting ribozymes will need to be continuously expressed to maintain a high level of mutant allele suppression. For this reason we stably transfected ribozyme constructs into OI fibroblasts to determine their effect on endogenous mutant α1(I) collagen mRNA. The 50% reduction in the level of mutant α1(I) collagen RNA observed in the OI G85V cells was higher than the 40% suppression we previously reported using antisense oligonucleotides targeted to α2(I) mRNA (5). More importantly, the ribozyme approach achieved a higher level of allele specificity in comparison to the antisense approach. Normal α1(I) mRNA levels were not significantly reduced when active or inactive ribozyme was expressed from vector pHβAPr-1-neo. A small (10–20%) but significant reduction was detected when either ribozyme was expressed from vector pCI.neo. This indicates a minimal antisense effect of the 13 nt binding arms but some influence of flanking vector sequence. From this observation we speculate that the vector sequences which surround the ribozyme may influence the cycling capacity of the ribozyme in the cellular environment. These findings may be important for designing ribozyme expression cassettes for future *in vivo* studies.

One limitation of the ribozyme gene therapy approach may be the level of mutant allele suppression required to achieve a therapeutic benefit. Our data demonstrate an ~50% reduction in the level of mutant α1(I) mRNA. There is currently no information available to determine if this level of suppression is sufficient to improve the phenotype of an affected OI patient, although complete suppression should not be necessary. Information on the required level of suppression can be obtained from studies of mutant type I collagen expression levels in bone of clinically mild mosaics who have a significant mutation burden at the tissue level. Mosaic individuals are suitable for such studies because gene therapy of dominantly inherited disorders is expected to create a somatic mosaic recipient. Furthermore, this study used human fibroblasts which express type I collagen under culture conditions. However, in the *in vivo* situation osteoblasts, known to express relatively higher levels of type I collagen than fibroblasts (19), will be the primary target cells. Thus, ribozymes would require a higher expression level or catalytic turnover in osteoblasts to achieve the same ratio of suppression as in fibroblasts. Second, the highly repetitive nature of the type I collagen helical sequence represents a challenge to antisense or ribozyme technologies which rely on stringent binding sites. Further studies are needed to evaluate whether modifications to ribozymes, such as varying the binding arm length to enhance cycling efficiency or adding collagen 3′-UTR sequences to enhance co-localization with mRNA, may improve the level of mutant allele suppression.

The efficiency of ribozymes for clinical purposes, for examples expression of ribozymes in osteoblast cells in OI patients, remains to be demonstrated. The data here reveal the ability of ribozymes to effect selective suppression of mutant α1(I) collagen mRNA in the cellular environment and provide a starting point on which *in vivo* applications of ribozymes can be based. In order to analyze the efficiency of ribozymes in the *in vivo* situation we have developed a knock-in mouse model of OI containing a typical OI mutation and a ribozyme cleavage site (20). To demonstrate efficacy of the ribozyme *in vivo* a transgenic mouse expressing the specific ribozyme has been generated and the therapy will initially be delivered by mating the ribozyme and OI mice. For future human trials one approach would be to transfect the patients' own marrow stromal cells *in vitro*, since this population is enriched for osteoblast precursors. The modified cells would be returned to the patient, generating a mosaic situation at the bone level. The optimum timing for such therapy would be during early childhood, when the improved new bone matrix could become a significant proportion of the tissue because of higher rates of bone deposition. Even transient expression of ribozyme (6–12 months) might theoretically have a positive effect on bone matrix mechanical properties and matrix–cell interactions.

ACKNOWLEDGEMENTS

Prof. G. Cetta supplied a sample of the OI G85V dermal fibroblasts. We thank Dr James Troendle for statistical analyses of cell growth rates and Peter Bouma for technical assistance with SDS–urea–PAGE. Finally, we acknowledge Dr Gabriele Grassi for useful discussions.

REFERENCES

1. Sillence,D.O. (1979) *J. Med. Genet.*, **16**, 101–116.
2. Marini,J.C. (1988) *Adv. Pediatr.*, **35**, 391–426.
3. Kuivaniemi,H., Tromp,G. and Prockop,D.J. (1997) *Hum. Mutat.*, **9**, 300–315.
4. Willing,M.C., Deschenes,S.P., Slayton,R.L. and Roberts,E.J. (1996) *Am. J. Hum. Genet.*, **59**, 799–809.
5. Wang,Q. and Marini,J.C. (1996) *J. Clin. Invest.*, **97**, 448–454.
6. Grassi,G. and Marini,J.C. (1996) *Trends Mol. Med.*, **28**, 499–510.
7. Yamada,O., Kraus,G., Leavitt,M.C., Yu,M. and Wong-Staal,F. (1994) *Virology*, **205**, 121–126.
8. Sun,L., Pytati,J., Smythe,J., Wang,L., MacPherson,J., Gerlach,W. and Symonds,G. (1995) *Proc. Natl Acad. Sci. USA*, **92**, 7272–7276.
9. Tang,X., Hobom,G. and Lao,D. (1994) *J. Med. Virol.*, **42**, 385–395.
10. Yamazaki,H., Kijima,H., Ohnishi,Y., Abe,Y., Oshika,Y., Tsuchida,T., Tokunaga,T., Tsugu,A., Ueyama,Y., Tamaoki,N. and Nakamura,M. (1998) *J. Natl Cancer Inst.*, **90**, 581–587.
11. Kilpatrick,M., Phylactou,L., Godfrey,M., Wu,C., Wu,G. and Tsipouras,P. (1996) *Hum. Mol. Genet.*, **5**, 1939–1944.
12. Montgomery,R.A. and Dietz,H.C. (1997) *Hum. Mol. Genet.*, **6**, 519–525.
13. Lewin,A.S., Drenser,K.A., Hauswirth,W.W., Nishikawa,S., Yasumura,D., Flannery,J.G. and LaVail,M.M. (1998) *Nature Med.*, **4**, 967–971.
14. Scherr,M., Grez,R., Ganser,A. and Engels,J.W. (1997) *J. Biol. Chem.*, **272**, 14304–14313.
15. Grassi,G., Forlino,A. and Marini,J.C. (1997) *Nucleic Acids Res.*, **25**, 3451–3458.
16. Valli,M., Zolezzi,F., Mottes,M., Antoniazzi,F., Stanzial,F., Tenni,R., Pignatti,P. and Cetta,G. (1993) *Eur. J. Biochem.*, **217**, 77–82.
17. Bonadio,J., Holbrook,K.A., Gelinas,R.E., Jacob,J. and Byers,P.H. (1985) *J. Biol. Chem.*, **260**, 1734–1742.
18. Millington-Ward,S., O'Neill,B., Kiang,A.-S., Humphries,P., Kenna,P.F. and Farrar,G.J. (1999) *Antisense Nucleic Acid Drug Dev.*, **9**, 537–542,
19. McCarthy,T.L., Centrella,M. and Canalis,E. (1988) *J. Bone Miner. Res.*, **3**, 401–406.
20. Forlino,A., Porter,F.D., Lee,E.J., Westphal,H. and Marini,J.C. (1999) *J. Biol. Chem.*, **274**, 37923–37931.